DALTON
FULL PAPER

# 1,2-Bis(2-benzimidazolyl)-1,2-ethanediol, a chiral, tridentate, facially coordinating ligand

**Katharina Isele,[a] Vanessa Broughton,[a] Craig J. Matthews,[a] Alan F. Williams,*[a] Gérald Bernardinelli,[b] Patrick Franz[c] and Silvio Decurtins[c]**

[a] *Département de Chimie Minérale, Analytique et Appliquée, Université de Genève, 30 quai Ernest Ansermet, CH 1211 Genève 4, Switzerland*
[b] *Laboratoire de Cristallographie aux Rayons-X, Université de Genève, 24 quai Ernest Ansermet, CH 1211 Genève 4*
[c] *Institut für Chemie und Biochemie, Universität Bern, Freiestrasse 3, CH 3012 Bern, Switzerland*

***Received 3rd April 2002, Accepted 1st August 2002***
***First published as an Advance Article on the web 16th September 2002***



The ligand 1,2-bis(1*H*-benzimidazol-2-yl)-1,2-ethanediol, **1**, and its methylated derivative **2** are readily synthesized from tartaric acid, and act as chiral, facially coordinating tridentate ligands, forming complexes of composition $ML_2$ with octahedral transition metals. The copper(II) complexes show distorted 4 + 2 coordination with benzimidazoles occupying the equatorial sites and alcohol functions weakly binding in the axial sites. Nickel(II) complexes in three different states of protonation show regular octahedral geometry with the alcohols mutually *cis*. Deprotonation of the coordinated alcohol produces little structural change but the monodeprotonated complex forms a hydrogen bonded dimer. Magnetic measurements show the hydrogen bonded bridge to offer a pathway for weak antiferromagnetic coupling. UV-Visible spectroscopy shows the ligand to have a field intermediate between water and pyridine. The diastereoselectivity of complexation depends on the geometry: nickel(II) shows a weak preference for the homochiral complex, whereas copper(II) forms almost exclusively homochiral complexes.

## Introduction

Ligands which occupy the coordination sites of a transition metal ion in a predictable way play an important role in modern coordination chemistry, since they may both define the number of reactive sites available at a metal centre and modulate their reactivity. Tridentate ligands may bind to an octahedral metal ion in a meridional or in a facial geometry. Terpyridyl (2,2′,6′,2″-terpyridine) is a well-known example of a meridional ligand, and 1,4,7-triazocyclononane (tacn) and the tris-pyrazolylborate family (categorized as scorpionates by Trofimenko) are good examples of facially coordinating ligands. Given the very rich chemistry of the tacn family[1] and the scorpionates,[2] the synthesis of new tridentate, facial ligands deserves attention. Such ligands should offer different types of binding site, and, with a view to enantioselective catalysis, the introduction of chirality in the ligands is an attractive prospect. The scorpionates and tacn ligands are generally achiral, although very recently a chiral version of tacn has been reported.[3] In this paper we report on the synthesis and coordination chemistry of 1,2-bis(1*H*-benzimidazol-2-yl)-1,2-ethanediol, **1**, and its methylated derivative **2** and show them to be readily synthesized and versatile chiral, tridentate facially coordinating ligands (Scheme 1).

The ligands **1** and **2** may be prepared by a simple Phillips reaction[4–6] from tartaric acid (either as the natural *RR*-form, or as the unnatural *SS*-enantiomer) with the appropriate 1,2-diaminobenzene. Despite the ease of synthesis, very little has been reported of the chemistry of this ligand: it has been mentioned in a study of inhibitors of rhinoviruses[7] and in connection with the enantioselective synthesis of cyanohydrins,[8] but the only report of complex formation concerned palladium(II) complexes where it acted as a bidentate ligand binding through the two benzimidazoles.[9,10] However, in a study of the related ligand 1,2-bis(2-benzimidazolyl)ethanol, **3**, formed using malic acid instead of tartaric acid, Reedijk and co-workers[11] showed that **3** could act as a facially coordinating tridentate ligand, with the alcohol group coordinated to nickel(II) in the octahedral complex $[Ni(\mathbf{3})_2]^{2+}$. Examination of the conformation of the ligand in the complexes [M(1,2-bis(2-benzimidazolyl)-ethane)$Cl_2$] (M = Mn, Cu)[12] suggested that the tartaric acid derivative should equally act as a tridentate ligand, with one alcohol group directed towards the metal and the second directed away, without significant distortion of the chelate ring. In this paper we show that ligands **1** and **2** do indeed act as chiral facially coordinating ligands and report on the chemistry of their complexes.

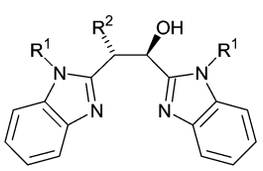


| | $R^1$ | $R^2$ |
|---|---|---|
| SS-**1** | H | OH |
| SS-**2** | $CH_3$ | OH |
| R-**3** | H | H |

**Scheme 1** Chemical structures of *SS*-**1**, *SS*-**2** and *R*-**3**.

## Results

### Syntheses and properties in solution

The ligands are prepared by simple Phillips condensation of the acid with the appropriate 1,2-diaminobenzene in 4 M hydrochloric acid. **1** is soluble in ethanol and DMSO, whereas **2** is poorly soluble in these solvents. Both ligands are insoluble in

**Table 1** Potentiometric titration data for the complexes (ethanol–water 1 : 1, 22 °C, $I = 0.1$ M)

| | **1** | | **2** | |
|---|---|---|---|---|
| | $\log_{10}(\beta_2)$ | $pK_{a1}$ | $\log_{10}(\beta_2)$ | $pK_{a1}$ |
| Co(II) | 7.6(1) | 6.5(2) | 8.2(1) | 7.6(2) |
| Ni(II) | 8.9(1) | 7.8(2) | 8.7(1) | 7.2(2) |
| Cu(II) | 12.2(1) | 5.9(2) | 11.8(1) | 6.6(2) |
| Zn(II) | 8.0(1) | 6.6(2) | 8.2(1) | 7.6(2) |

water. The complexes are formed by reaction with metal salts in alcohol, DMSO or acetonitrile solution. Unless specifically stated to the contrary, experiments used the enantiopure *SS* ligand. Spectroscopic titrations in DMSO showed clearly the formation of complexes of composition M(ligand)$_2$, and this was confirmed by electrospray mass spectrometry and potentiometric titrations in 1 : 1 ethanol–water (M = Co, Ni, Cu, Zn) (Table 1). The results are independent of the chirality of the ligand used.

The potentiometric titrations also showed that deprotonation of the complexes occurred at neutral pH or higher. Titration curves for the nickel complexes are shown in Fig. 1. Ligands

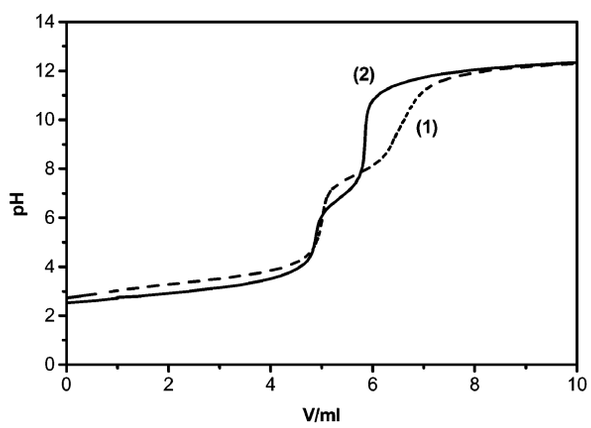


**Fig. 1** Titration curves of Ni(II) with **1** (dashed line) and **2** (full line) using 0.1 M NaOH.

**1** and **2** may be deprotonated at the alcohol function, or, for ligand **1**, at the benzimidazole hydrogen, and both groups become more acid upon complexation to a metal ion. Since deprotonation was observed at similar pH values for complexes of **1** and **2**, we deduce that the initial deprotonation takes place at the alcohol function which must therefore be coordinated to allow deprotonation around pH 6–8. The curves for ligand **2** generally show two deprotonations, and precipitation was frequently observed after the second deprotonation. The curves for ligand **1** were less well resolved, suggesting that at higher pH benzimidazole deprotonation may equally occur. For cobalt and nickel, the second deprotonation of complex **2** was not observed before pH 10, and we attribute this to the stabilisation of the second alcohol proton due to the formation of the hydrogen bridged dimer $\{[M_2(\mathbf{2})_2(\mathbf{2}\text{-H})_2]_2\}^{2+}$ whose crystal structure is discussed below. This was confirmed by electrospray mass spectrometry, which also showed that at higher pH complexes of ligand **1** showed a strong tendency to form polynuclear complexes which will be discussed in a subsequent paper. The stoichiometry of complex formation and the coordination of the alcohol establish these ligands as tridentate.

The salts of the complexes $ML_2$ were synthesised by mixing metal salts and ligands in the appropriate quantities and crystallising.

For the monodeprotonated complexes of cobalt and nickel crystallisation was carried out after addition of one equivalent of base (sodium hydroxide) per metal. The doubly deprotonated nickel compound was obtained from a solution of $[Ni(SS\text{-}\mathbf{2})_2]^{2+}$ to which an excess of base had been added. Blue crystals of $[Ni(SS\text{-}\mathbf{2}\text{-H})_2]\cdot 4H_2O\cdot C_2H_5OH$ formed slowly in the initially formed amorphous green precipitate, and a specimen crystal was analysed by X-ray crystallography.

## Crystal structures

The crystal structures of the complexes $[Cu(SS\text{-}\mathbf{1})_2](ClO_4)_2$ and $[Cu(SS\text{-}\mathbf{2})_2](ClO_4)_2$ are very similar, and show the ligands to bind in a tridentate facial manner (Fig. 2).

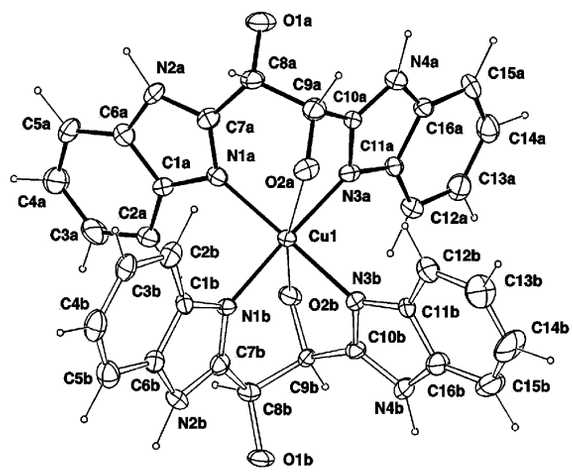


**Fig. 2** Structure of the cation $[Cu(SS\text{-}\mathbf{1})_2]^{2+}$ showing the tridentate facial coordination of the ligand. Ellipsoids are represented with 40% probability.

As one would expect, the coordination of the copper ions is strongly distorted from octahedral: the four nitrogen donor atoms of the ligands coordinate the copper in a square planar manner with average Cu–N distances of 2.01 Å, and N–Cu–N angles close to 90°, with the coordinated alcohol functions much more weakly bound (average distance 2.51 Å) in the axial positions, and thus mutually *trans*. However, the Cu–O bonds are not perpendicular to the $CuN_4$ plane, but are displaced towards the two nitrogens of the same ligand. The differences in geometry between the two structures are not significant. The conformation of the seven-membered chelate ring is essentially the same as in the complexes of 1,2-bis(2-benzimidazolyl)-ethane,[12] showing that coordination of the alcohol function has not distorted the seven-membered chelate ring.

The conformation of the ligands requires the planes of the two benzimidazoles of each ligand to be inclined at about 100° to each other: the complex as a whole has a structure which may be described as a capital X, with the copper at the centre and the benzimidazoles forming the vertical arms. This determines the crystal packing, in which the complexes lie in sheets with stacking interactions between the benzimidazoles. The anions lie in between the sheets of cations. A similar type of interaction has been observed in the crystal chemistry of bis-terpy metal complexes.[13] The uncoordinated alcohol functions and the NH groups of **1** are involved in hydrogen bonding to the anions and solvent.

Structures have been determined for the nickel complexes in three different states of protonation. In all cases the ligand binds facially, with the two coordinated alcohol functions mutually *cis* (Figs. 3 and 4) and the complex shows crystallographic two-fold symmetry. The fully protonated structure was determined for the complex formed from a racemate of the ligand, and showed the formation of homochiral complexes $[Ni(RR\text{-}\mathbf{1})_2]^{2+}$ and $[Ni(SS\text{-}\mathbf{1})_2]^{2+}$ as observed for ligand **3** by Reedijk.[11] The monodeprotonated complex shows a dimeric

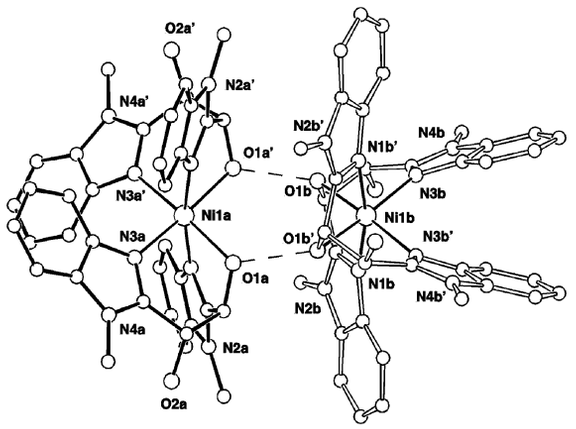


**Fig. 3** View of the dimer $[Ni(RR\text{-}\mathbf{2})_2Ni(RR\text{-}\mathbf{2}\text{-}H)_2]^{2+}$ showing the *cis* arrangements of the coordinated alcohols and the two O ··· H–O forming the dimer. Primed atom symmetry: $x$, $1 - y$, $1 - z$ (horizontal $C_2$ axis).

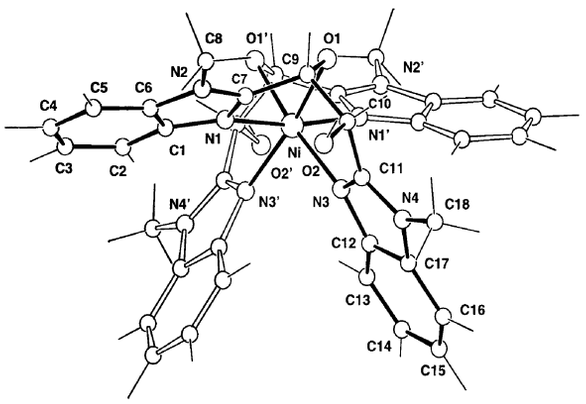


**Fig. 4** Structure of the complex $[Ni(SS\text{-}\mathbf{2}\text{-}H)_2]$. Primed atom symmetry: $x$, $y$, $-z$ (vertical $C_2$ axis).

structure which should formally be described as $[Ni(RR\text{-}\mathbf{2})_2Ni(RR\text{-}\mathbf{2}\text{-}H)_2]^{2+}$ in which the coordinated alcohols of one complex hydrogen bond to the coordinated alkoxides of the other. This stabilises the monodeprotonated form and explains the relative difficulty in effecting the second deprotonation of the complex $[Ni(\mathbf{2})_2]^{2+}$ mentioned above (Fig. 3). However, this formulation may be a consequence of the crystallographic two-fold axis, and may not be valid in solution. The nickel–nickel distance in the dimer is 5.055(3) Å.

The geometries of the three complexes are very similar and show only slight changes in bond distances and angles. The Ni–N1 distances increase with deprotonation in the order 2.054(2), 2.075(15), 2.075(7) Å, as do the Ni–N3 distances *trans* to the coordinated oxygens in the order 2.080(2), 2.105(8), 2.136(6) Å. The Ni–O distances change irregularly: 2.160(2), 2.068(8), 2.103(5) Å. Bond angles change little: the N1–Ni–N3 chelate angle falls slightly upon deprotonation from 95.04(9) to 93.3(3)° in the fully deprotonated complex. The N1–Ni–O1 angle ranges from 77.02(8) to 80.5(3)°, and the N3–Ni–O1 angle is slightly larger [range 81.9(2)–83.21(7)°]. The values agree well with those reported by Reedijk.[11]

The crystal packing of *rac*-$[Ni(RR,SS\text{-}\mathbf{1})_2](NO_3)_2(C_2H_5OH)_2$ shows layers of cations in the *bc* plane in which complexes of alternating chirality are held together by stacking interactions between benzimidazoles related by a centre of inversion. The OH and NH functions of the ligand are involved in extensive hydrogen bonding with the anions and solvent molecules. For $[Ni(RR\text{-}\mathbf{2})_2Ni(RR\text{-}\mathbf{2}\text{-}H)_2](ClO_4)_2(C_2H_5OH)_3$, the layers of cations lie in the *ab* plane, but no intermolecular stackings are observed. The crystal packing of the neutral complex $[Ni(SS\text{-}\mathbf{2}\text{-}H)_2]$ is quite different: the complexes are arranged around the $3_1$ axis with the two deprotonated alcohol functions directed towards the axis. There is a network of hydrogen bonds involving alkoxides, uncoordinated alcohols and included solvent molecules. No stacking is observed (Fig. 4).

## Magnetic measurements

The observation of a hydrogen bridged dimer for $[Ni(RR\text{-}\mathbf{2})(RR\text{-}\mathbf{2}\text{-}H)]_2^{2+}$ suggested a possible pathway for magnetic interaction between the two nickel ions. The magnetic susceptibilities of the dimer $[Ni(RR\text{-}\mathbf{2})_2Ni(RR\text{-}\mathbf{2}\text{-}H)_2]^{2+}$ and the equivalent mononuclear compound *rac*-$[Ni(RR,SS\text{-}\mathbf{1})_2](NO_3)_2(C_2H_5OH)_2$ were therefore studied in the temperature range 2–300 K, and the results are shown in Fig. 5. The monomeric

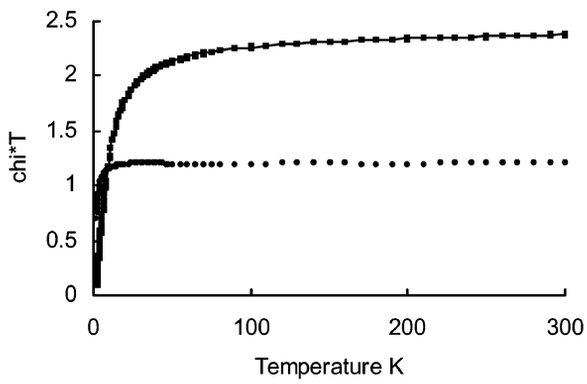


**Fig. 5** Observed values of $\chi T$ for $[Ni(RR\text{-}\mathbf{2})_2]^{2+}[Ni(RR\text{-}\mathbf{2}\text{-}H)_2]^2$ (■) and $[Ni(\mathbf{1})_2]^{2+}$ (●). A simulated curve for a coupled dimer of nickel ions with $g = 2.154$, $J = -4.7$ cm$^{-1}$ and a temperature independent paramagnetism of $3.3 \times 10^{-4}$ cm$^3$ mol$^{-1}$ is shown for the dimer.

compound shows the expected curve for a $S = 1$ paramagnetic system, the product $\chi T$ dropping off only below 10 K. The dimer shows a fall in $\chi T$ at much higher temperatures, in agreement with an antiferromagnetic coupling between the two centres. A least squares fit to $\chi T$ of a coupled system using an isotropic Hamiltonian $H = -J\boldsymbol{S}_A\cdot\boldsymbol{S}_B$ gave a good fit with a $J$ value of $-4.7$ cm$^{-1}$. This is rather smaller than the value reported very recently for a dimer of copper(II) equally formed by two O ··· H–O hydrogen bonds, where a value of 21 cm$^{-1}$ was reported.[14] Although the hydrogen bond is shorter in the nickel complex [2.399(7) compared with 2.596(3) Å] the total metal–metal distance is greater [5.055(3) compared to 4.736(2) Å]. We conclude that, although the hydrogen bond does offer a path for antiferromagnetic coupling, the effect is quite small.

## Electronic spectra

The spectra in solution will be discussed firstly for the nickel complexes which have been characterised by X-ray crystallography. The electronic spectra and circular dichroism spectra are reported in Tables 2 and 3.

The nickel complexes show the expected three d–d transitions for an octahedral complex (Fig. 6). The spectra were essentially identical in acetonitrile and in ethanol. The racemate spectrum in *rac*-$[Ni(RR,SS\text{-}\mathbf{1})_2](NO_3)_2(C_2H_5OH)_2$ in DMSO solution gave an identical spectrum to the optically pure samples, and its reflectance in a MgO matrix showed peaks at the same energies as the solution spectrum. On the basis of the position of the first d–d band, the ligand field splitting in $[Ni(\mathbf{1})_2]^{2+}$ is 10000 cm$^{-1}$, fairly close to what would be expected using a weighted average of Jørgensen's ligand field factors for water and pyridine.[15] Deprotonation of the complex produces only slight shifts in the band positions, as would be expected for deprotonation of the alcohol functions.

**Table 2** d–d Transitions ($\lambda_{max}$, $\varepsilon$) for the nickel, cobalt and copper complexes, recorded in acetonitrile

| $[Ni(\mathbf{1})_2]^{2+}$ | $[Ni(\mathbf{2})_2]^{2+}$ | $[Ni_2(\mathbf{2})_2(\mathbf{2}\text{-H})_2]^{2+}$ | Assignment |
|---|---|---|---|
| 999(6.5) | 988(6.6) | 961(8.3) | $^3T_2 \longleftarrow {}^3A_2$ |
| 595(16) | 590(19) | 576(8.6) | $^3T_1 \longleftarrow {}^3A_2$ |
| 376(22) | 377(25) | 367(17) | $^3T_1 \longleftarrow {}^3A_2$ |
| $[Co(\mathbf{1})_2]^{2+}$ | $[Co(\mathbf{2})_2]^{2+}$ | $[Co_2(\mathbf{2})_2(\mathbf{2}\text{-H})_2]^{2+}$ | Assignment |
| 1132(12) | 1131(16) | 1061(8) | $^4T_2 \longleftarrow {}^4T_1$ |
| 601sh(18) | 603sh(29) | | $^4A_2 \longleftarrow {}^4T_1$ |
| 506(89) | 505(133) | | |
| 486(85) | 485(126) | 476(30) | $^4T_1 \longleftarrow {}^4T_1$ |
| 468(82) | 466(122) | | |
| $[Cu(\mathbf{1})_2]^{2+}$ | $[Cu(\mathbf{2})_2]^{2+}$ | | |
| 681(23) | 683(29) | | |
| 569(26) | 567(33) | | |

**Table 3** Circular dichroism (CD) ($\lambda_{max}$, $\Delta\varepsilon$) spectra for the nickel, cobalt and copper complexes, recorded in acetonitrile

| $[Ni(RR\text{-}\mathbf{1})_2]^{2+}$ | $[Ni(RR\text{-}\mathbf{2})_2]^{2+}$ | $[Ni_2(RR\text{-}\mathbf{2})_2(\mathbf{2}\text{-H})_2]^{2+}$ |
|---|---|---|
| 750sh(−0.094) | 760sh(−0.090) | 755(−0.057) |
| 684(−0.228) | 690(−0.261) | 662(+0.024) |
| 396(−0.124) | 396(−0.142) | 563(−0.081) |
| 358(+0.126) | 358(+0.144) | 384(−0.070) |
| $[Co(RR\text{-}\mathbf{1})_2]^{2+}$ | $[Co(SS\text{-}\mathbf{2})_2]^{2+}$ | $[Co_2(SS\text{-}\mathbf{2})_2(\mathbf{2}\text{-H})_2]^{2+}$ |
| 604(−0.217) | 612(+0.251) | 519sh(−0.182) |
| 484(+0.287) | 476(−0.435) | 492(−0.270) |
| 459(+0.369) | 456(−0.440) | 450(−0.244) |
| $[Cu(SS\text{-}\mathbf{1})_2]^{2+}$ | $[Cu(SS\text{-}\mathbf{2})_2]^{2+}$ | |
| | 700sh(−0.081) | |
| 588(−0.448) | 590(−0.415) | |
| 501(+0.096) | 502(+0.076) | |

The circular dichroism spectra are normal for the mononuclear complexes, showing a negative band around 700 nm, probably associated with the spin forbidden transition to the $^1E$ state. For instrumental reasons, it was not possible to measure the CD of the first allowed d–d transition, but a positive rise was observed at 900 nm, the longest wavelength accessible. The CD spectrum of the hydrogen bonded dimer is quite different from the monomers (Fig. 6).

The cobalt complexes are consistent with high spin octahedral cobalt(II); the second spin-allowed d–d band often appears as structured with three bands of approximately equal intensity. The copper complexes gave a broad band with two maxima, consistent with the 4 + 2 coordination observed in the solid state.

### Diastereoselectivity of complex formation

Complexes of the type $ML_2$ with racemates of chiral ligands may exist either as racemic mixtures of the homochiral complexes ($[M(RR\text{-}L)_2]$ and $[M(SS\text{-}L)_2]$) or as the heterochiral complex $[M(RR\text{-}L)(SS\text{-}L)]$.[16] We have studied the diastereoselectivity of complex formation by **1** with copper(II) and nickel(II) where the stereochemistry of complexation is quite different. For the nickel complex, the crystal structure of

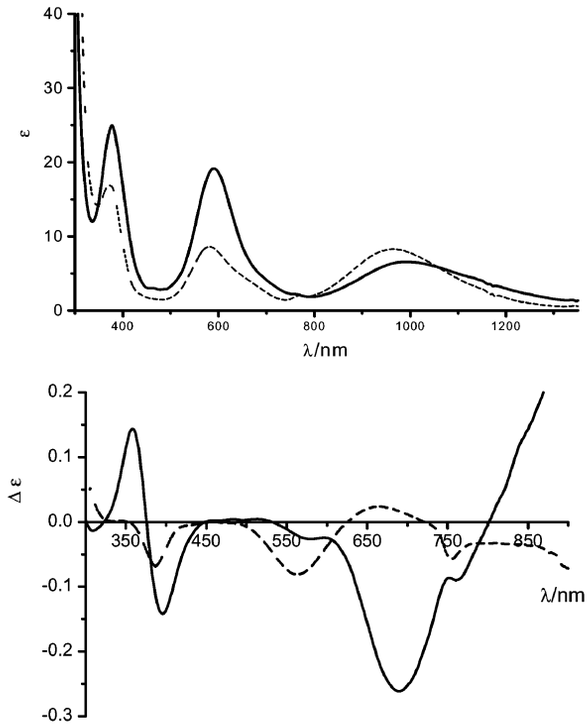


**Fig. 6** Electronic spectra and CD of the complexes $[Ni(RR\text{-}\mathbf{2})_2]^{2+}$ (full line) and $[Ni_2(RR\text{-}\mathbf{2})_2(RR\text{-}\mathbf{2}\text{-H})_2]^{2+}$ (dashed line) in acetonitrile solution.

*rac*-$[Ni(RR,SS\text{-}\mathbf{1})_2](NO_3)_2(C_2H_5OH)_2$ showed only the homochiral complex, but this may be an artefact of the crystallisation process, and is not necessarily a measure of the diastereomeric distribution in solution. Bernauer and collaborators[17] have shown that study of the circular dichroism spectrum of solutions as the ratio of *RR*-ligand to *SS*-ligand is varied allows the measurement of the diastereoselectivity *S* (defined as the ratio of formation constants $K_{meso}/2K_{rac}$). A value of *S* greater than one implies greater stability of the heterochiral *meso* form, and $S < 1$ implies a preference for the formation of the homochiral species. The experimental points together with the fitted curves for the value of *S* are shown in Fig. 7. For the

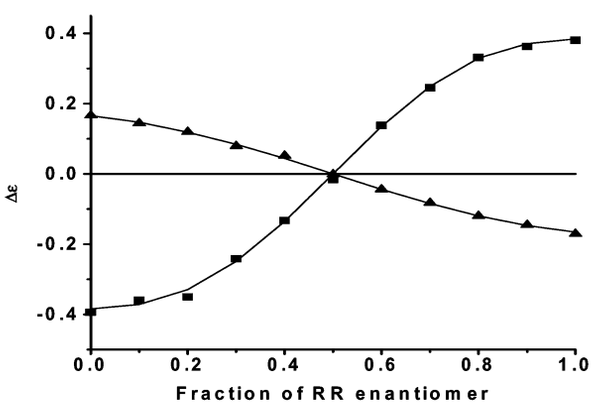


**Fig. 7** Variation of the molar ellipticity as a function of the *SS*/*RR* ratio for the nickel(II) (▲) and copper(II) (■) complexes.

nickel complex a value of *S* of 0.44(1) was obtained in DMSO solution, implying a weak preference for the homochiral form, which is indeed observed in the solid state. For the copper complex however, a value of 0.01(2) was obtained, showing virtually complete formation of the homochiral complex. This dramatic difference in diastereoselectivity is presumably related to the different coordination geometries in the two cases.

## Experimental

### Physical measurements

Potentiometric titrations were carried out in 1 : 1 water–ethanol mixtures. In a typical experiment ligand (0.2 mmol), metal (0.1 mmol) and HCl (0.5 mmol) were dissolved in a volume of 40 ml, with ionic strength adjusted to 0.1 M with sodium chloride. The solutions were titrated with NaOH (0.1 M) with a Mettler DL70 titrator at 22 °C in a nitrogen atmosphere. The pH data were fitted to the equilibrium model with a local version of the TITFIT program[18] allowing the dissociation constant for water to vary to allow for the non-aqueous solvent. The protonation constants $\log_{10}(\beta_1)$ and $\log_{10}(\beta_2)$ were determined to be 5.01(4) and 8.79(6) for **1** and 4.46(6) and 8.50(9) for **2**. Electronic spectra were recorded using a Perkin-Elmer Lambda 900 UV/VIS/NIR spectrometer, CD spectra using a Jasco J-715 spectropolarimeter and infra-red spectra as KBr pastilles using a Perkin-Elmer Spectrum One spectrometer. NMR spectra were recorded on a Varian Gemini instrument, at 300 MHz for protons and 75.44 MHz for $^{13}$C. Reflectivity spectra were recorded using a Perkin-Elmer Lambda 900 UV/VIS/NIR spectrometer equipped with an integration sphere of diameter 60 mm. The white standard was PTFE. Samples were prepared in a 1 mm cell after mixing the compound with magnesium oxide (~10% compound). Baseline correction was performed by measuring the spectrum of pure magnesium oxide. Magnetic susceptibility data were collected with a Quantum Design SQUID magnetometer (XL5S) operating in the temperature range 300–2 K with a field of 1000 Gauss. Pascal's constants[19] were used for the diamagnetic corrections. The experimental data for $\chi T$ were fitted to the equation

$$\chi T = \frac{2Ng^2\beta^2}{k}\left[\frac{e^x + 5e^{3x}}{1 + 3e^x + 5e^{3x}}\right] + \alpha T$$

where $x = -J/kT$. The r.m.s. error on the fit was 0.014 cm$^3$ mol$^{-1}$ K.

### Synthesis of the ligands

**(*R*,*R*)-1,2-Bis(1*H*-benzimidazol-2-yl)-1,2-ethanediol (*RR*-1).** 1,2-Phenylenediamine (10.00 g, 92.5 mmol) and D(−) tartaric acid (6.94 g, 46.3 mmol) were dissolved in 200 ml 4 M hydrochloric acid. The solution was heated to reflux for 24 hours. On cooling, green crystals of the chloride salt of the protonated ligand formed. The crystals were filtered and dissolved in 200 ml water and treated with activated carbon under reflux for 2 hours. Neutralisation with concentrated ammonia gave a white voluminous precipitate. The precipitate, was filtered and recrystallised from a water–ethanol mixture (200 ml–200 ml) to give colourless needles or plates of (*RR*)-1,2-bis(1*H*-benzimidazol-2-yl)-1,2-ethanediol (*RR*-**1**) (3.41 g, 25%) (Found: C, 63.23; H, 4.95; N, 18.13. $C_{16}H_{14}N_4O_2\cdot 0.5H_2O$ requires C, 63.35; H, 4.99; N, 18.48%); UV ($T$ = 22 °C/3.14 × 10$^{-4}$ M/DMSO/$l$ = 1 mm) $\lambda_{max}$/nm ($\varepsilon$/dm$^3$ mol$^{-1}$ cm$^{-1}$) 250 (13100), 278 (18300), 283 (17400); CD ($T$ = 22 °C/3.14 × 10$^{-4}$ M/DMSO/$l$ = 1 mm) $\lambda_{max}$/nm ($\Delta\varepsilon$/dm$^3$ mol$^{-1}$ cm$^{-1}$): 248 (0.704), 261 (−0.072), 281 (−0.140), 288 (−0.220); IR (KBr) $\nu$/cm$^{-1}$ 3200br, 3385s, 3330m, 3058m, 1620m, 1590m, 1527m, 1483m, 1454s, 1430w, 1307m, 1272w, 1226m, 1205m, 1111m, 1086s, 1059m, 1030s, 997m, 899m, 844m, 796m, 763s, 738m, 613m, 439m, 360m; NMR [DMSO-d$_6$] $\delta_H$ (300 MHz) 12.33 (br s, NH, 2H), 7.49 (m, arom. H, 4H), 7.12 (m, arom. H, 4H), 5.92 (d, OH, 2H, $J$ = 5 Hz), 5.28 (d, CH, 2H, $J$ = 5 Hz); $\delta_C$ (75.44 MHz) 156.29 (C=N), 143.82 (arom. C), 134.73 (arom. C), 122.18 (arom. C), 121.60 (arom. C), 119.04 (arom. C), 112.09 (arom. C), 71.60 (CH); MS (EI 70 eV) $m/z$ 294 (M$^+$), 148, 119, 65. Solubility: soluble in DMSO, DMF; poorly soluble in ethanol and methanol, insoluble in $H_2O$, $CH_3CN$. The enantiomeric ligand *SS*-**1** was prepared by a similar route.

**(*S*,*S*)-1,2-Bis(1-methylbenzimidazol-2-yl)-1,2-ethanediol (*SS*-2).** *N*-Methyl-1,2-phenylenediamine [5 ml (97%), 42.7 mmol] and L(+) tartaric acid (3.21 g, 21.3 mmol) were dissolved in 50 ml 4 M hydrochloric acid. The solution was heated to reflux for 24 hours. After cooling, a blue compound (the chloride salt of the protonated ligand) crystallised from the black solution. The crystals were filtered and redissolved in 150 ml water and 150 ml ethanol. After adding active carbon the solution was heated to reflux for 2 hours. The colourless solution was neutralised with conc. ammonia and the white precipitate was filtered. Recrystallisation was difficult due to the low solubility of the compound. To recrystallise 0.265 g of **2** a volume of 500 ml (4 : 1 ethanol–water) was necessary. An alternative is to dissolve the product in water–ethanol (230 ml–150 ml) and conc. HCl (53 ml) and to heat to reflux in the presence of active carbon. After cooling, the protonated ligand crystallises. The precipitate is filtered and redissolved in 200 ml water and 200 ml ethanol. The hot solution is neutralised slowly by sodium hydroxide (5 M). The solution with the white precipitate was allowed to cool and then filtered. The precipitate of (*S*,*S*)-1,2-bis(1-methylbenzimidazol-2-yl)-1,2-ethanediol (*SS*-**2**) was dried in a oven at 90 °C for several hours; (3.98 g, 58%) (Found: C, 66.89; H, 5.66; N, 17.35. $C_{18}N_4O_2H_{18}$ requires C, 67.10; H, 5.59; N, 17.38%); UV ($T$ = 22 °C/3.14 × 10$^{-4}$ M/DMSO/$l$ = 1 mm) $\lambda_{max}$/nm ($\varepsilon$/dm$^3$ mol$^{-1}$ cm$^{-1}$) 248 (16100), 258 (15200), 273 (14400), 279 (15800), 287 (13400); CD ($T$ = 22 °C/3.14 × 10$^{-4}$ M/DMSO/$l$ = 1 mm) $\lambda_{max}$/nm ($\Delta\varepsilon$/dm$^3$ mol$^{-1}$ cm$^{-1}$) 251 (0.521), 264 (−1.520), 274 (−1.231), 290 (0.865); IR (KBr) $\nu$/cm$^{-1}$ 3097w, 2850w, 1614s, 1589m, 1481m, 1397s, 1345m, 1329m, 1310s, 1281s, 1243s, 1145s, 1108s, 1075s, 1002s, 911s, 873m, 845m, 799m, 767s, 731m, 657m, 576m, 536s, 445m, 380s; NMR [DMSO-d$_6$] $\delta_H$ (300 MHz) 7.45 (m, arom. H, 4H), 7.10 (m, arom. H, 4H), 6.09 (m, OH, 2H), 5.44 (m, CH, 2H), 3.91 (s, $CH_3$, 6H); $\delta_C$ (75.44 MHz) 154.90 (C=N), 142.19 (arom. C), 136.14 (arom. C), 122.66 (arom. C), 121.89 (arom. C), 119.52 (arom. C), 110.65 (arom. C), 67.92 (CH), 30.55 ($CH_3$); MS (EI 70 eV): $m/z$ = 323 (M$^+$), 304, 275, 162, 92, 77. Solubility: insoluble in most organic solvents and $H_2O$, weakly soluble in DMSO, hot ethanol, hot methanol. The enantiomeric ligand *RR*-**2** was prepared by a similar route.

### Synthesis of the complexes

**CAUTION!** Perchlorate salts of organic ligands are potentially explosive. Only small amounts should be used and suitable protective measures should be taken.[20]

***Rac*-bis[1,2-bis(1*H*-benzimidazol-2-yl)-1,2-ethanediol]-nickel(II) dinitrate, *rac*-[Ni(*RR*,*SS*-1)$_2$](NO$_3$)$_2$(C$_2$H$_5$OH)$_2$.** A mixture of $Ni(NO_3)_2\cdot 6H_2O$ (0.0291 g, 0.1 mmol), *RR*-**1** (0.0294 g, 0.1 mmol) and *SS*-1 (0.0294 g, 0.1 mmol) was dissolved in 2.5 ml ethanol and 0.25 ml water. Slow evaporation of half of the solvent led within a week to blue prismatic crystals. The solution was filtered and the crystals washed with water and dried in air (0.0661 g, 77%); (Found: C, 49.7; H, 4.5; N, 16.53. $C_{32}H_{28}N_8O_4\cdot Ni(NO_3)_2\cdot CH_3CH_2OH$ requires C, 50.1; H, 4.7; N, 16.2%; UV ($T$ = 22 °C/0.029 M/DMSO) $\lambda_{max}$/nm ($\varepsilon$/dm$^3$ mol$^{-1}$ cm$^{-1}$) 993 (6), 594 (12), 376(18); Reflectivity in MgO $\lambda_{min}$/nm 993; IR (KBr) $\nu$/cm$^{-1}$ 3206br s, 1765m, 1623s, 1594s, 1549m, 1532m, 1416br s, 1274m, 1149s, 1119s, 1067m, 1037m, 1004s, 986s, 924s, 908s, 879s, 822s, 810s, 765s, 740m, 633s, 620s, 577m, 510m, 483s, 453s, 437s, 426s; ES-MS (DMSO) : $m/z$ (%) 362.3 (100) [Ni(**1**)$_2$(DMSO)]$^{2+}$, 323.3 (74) [Ni(**1**)$_2$]$^{2+}$, 401.3 (56) [Ni(**1**)$_2$(DMSO)$_2$]$^{2+}$, 295.1 (45) [(**1**)H]$^+$, 429.1 (22) [Ni(**1** − H)]$^+$(DMSO), 440.2 (13) [Ni(**1**)$_2$(DMSO)$_3$]$^{2+}$, 645.1 (13) [Ni(**1**)$_2$(−H)]$^+$.

**Bis[bis[(*R*,*R*)-1,2-bis(1-methylbenzimidazol-2-yl)-1,2-ethanediol]nickel(II) diperchlorate, [Ni(*RR*-2)(*RR*-2-H)]$_2$(ClO$_4$)$_2$(C$_2$H$_5$OH)$_3$.** A mixture of $Ni(ClO_4)_2\cdot 6H_2O$ (0.0366 g, 0.1 mmol) and *RR*-**2** (0.0644 g, 0.2 mmol) was dissolved in 25 ml ethanol to

give a blue solution. Adding one equivalent of hydroxide (100 μl of 1 M NaOH) led to a turbid pale violet solution which became clear again when 4 ml water were added. After 9 days of slow evaporation pale violet crystals in the form of prisms formed. The solution was filtered and the crystals washed with ethanol and dried in air (0.0705 g, 81%); (Found: C, 53.35; H, 5.1; N, 12.5. $C_{72}H_{70}N_{16}O_8{\cdot}2Ni{\cdot}2ClO_4{\cdot}3CH_3CH_2OH$ requires C, 53.8; H, 5.1; N, 12.9%); UV ($T$ = 22 °C/0.019 M/acetonitrile) $\lambda_{max}$/nm ($\varepsilon$/dm$^3$ mol$^{-1}$ cm$^{-1}$) 961 (8), 576 (8), 368 (15); CD ($T$ = 22 °C/0.019 M/acetonitrile) $\lambda_{max}$/nm ($\Delta\varepsilon$/dm$^3$ mol$^{-1}$ cm$^{-1}$) 754 (−0.056), 665 (0.024), 562 (−0.079), 385 (−0.069); Reflectivity in MgO $\lambda_{min}$/nm 955, 575, 370; IR (KBr) $\nu$/cm$^{-1}$ 3418br s, 3057m, 2953m, 2882m, 1615s, 1480m, 1454m, 1416m, 1326m, 1289s, 1236m, 1103w, 1009s, 930m, 836m, 813s, 746m, 686s, 622s, 563s, 547s, 504m, 442s, 428s; ES-MS (acetonitrile): $m/z$ (%) 323.2 (100) [(**2**)H]$^+$, 701.0 (36) [Ni$_2$(**2**)$_4$(−2H)]$^{2+}$, 541.0 (36) [Ni$_2$(**2**)$_3$(−2H)]$^{2+}$, 1503.6 (23) [Ni$_2$(**2**)$_4$(−2H)(ClO$_4$)]$^+$, 801.0 (12) [Ni(**2**)$_2$(ClO$_4$)]$^+$, 1181.3 (10) [Ni$_2$(**2**)$_3$(−2H)(ClO$_4$)]$^+$, 379.1(10) [Ni(**2**)(−H)]$^+$.

**Bis[(*S*,*S*)-1,2-bis(1-methylbenzimidazol-2-yl)-1,2-ethanediolate]nickel(II), [Ni(*SS*-2-H)$_2$](H$_2$O)$_4$(C$_2$H$_5$OH).** A mixture of Ni(ClO$_4$)$_2{\cdot}6$H$_2$O (0.0366 g, 0.1 mmol) and *SS*-**2** (0.0644 g, 0.2 mmol) dissolved in 4 ml ethanol and 1 ml water gave a blue solution. The colour of the solution turned to green when 10 equivalents hydroxide (1 ml of 1 M NaOH) were added. Slow evaporation led to blue prismatic crystals in a green amorphous precipitate. Precipitation started within two days (0.008 g, 10%); (Found: C, 55.9; H, 5.9; N, 13.3. $C_{36}H_{34}N_8O_4{\cdot}Ni{\cdot}4H_2O{\cdot}CH_3CH_2OH$ requires C, 53.8; H, 5.1; N, 12.9%).

**Bis[(*S*,*S*)-1,2-bis(1*H*-benzimidazol-2-yl)-1,2-ethanediol]-copper(II) diperchlorate, [Cu(*SS*-1)$_2$]$_2$(ClO$_4$)$_4$(CH$_3$CN)$_4$(CH$_2$-Cl$_2$).** A solution of copper(II) perchlorate hexahydrate (0.141 g, 0.38 mmol) in acetonitrile (10 ml) was added to a suspension of *SS*-**1** (0.224 g, 0.76 mmol) in acetonitrile (30 ml) with stirring at room temperature. After 1 h a clear green solution formed which was reduced *in vacuo* (8 ml). The product was crystallised *via* slow vapour diffusion of dichloromethane to yield pale blue cubic crystals. The product was recrystallised in the same manner described above, filtered, and dried in air (0.171 g, 53%); (Found: C, 42.0; H, 3.8; N, 12.3. $C_{32}H_{28}N_8O_4{\cdot}Cu(ClO_4)_2{\cdot}H_2O{\cdot}0.5CH_3CN$ requires C, 42.0; H, 3.5; N, 12.3%); IR (KBr) $\nu$/cm$^{-1}$ 3238br s, 1621m, 1593m, 1472m, 1452s, 1330m, 1274m, 1211w, 1089s, 921w, 877w, 744s, 627s, 458w, 429w, 351w.

**Bis[(*S*,*S*)-1,2-bis(1-methylbenzimidazol-2-yl)-1,2-ethanediol]copper(II) diperchlorate, [Cu(*SS*-2)$_2$](ClO$_4$)(CH$_3$OH)$_2$-(H$_2$O)$_{1.5}$.** A mixture of Cu(ClO$_4$)$_2{\cdot}6$H$_2$O (0.0371 g, 0.2 mmol) and *SS*-**2** (0.0644 g, 0.2 mmol) was dissolved in 16 ml methanol and 6 ml ethanol. The turquoise solution was slowly evaporated. Within one day blue–violet crystals began to grow. After one week the solution was filtered and the crystals washed in ethanol and dried in air (0.0770 g, 79.7%); (Found: C, 44.0; H, 4.3; N, 11.4. $C_{36}H_{36}N_8O_4{\cdot}Cu(ClO_4)_2{\cdot}4H_2O$ requires C, 44.0; H, 4.6; N, 11.4%). UV ($T$ = 22 °C/0.013 M/acetonitrile) $\lambda_{max}$/nm ($\varepsilon$/dm$^3$ mol$^{-1}$ cm$^{-1}$) 574 (29), 686sh (21); CD ($T$ = 22 °C/0.013 M/acetonitrile) $\lambda_{max}$/nm ($\Delta\varepsilon$/dm$^3$ mol$^{-1}$ cm$^{-1}$) 506 (0.092), 595 (−0.431); IR (KBr) $\nu$/cm$^{-1}$ 3381br s, 2953m, 1614m, 1596s, 1504m, 1483m, 1457m, 1417m, 1334m, 1286m, 1264m, 1111w, 929s, 912s, 839s, 811s, 753m, 690m, 622m, 563s, 518s, 496m, 430m, 401m; ES-MS (acetonitrile) $m/z$ (%) 353.6 (100) [Cu(**2**)$_2$]$^{2+}$, 385.0 (42) [Cu(**2**)(−H)]$^+$, 323.1 (32) [(**2**)H]$^+$, 426 (15) [Cu(**2**)(−H)(CH$_3$CN)]$^+$, 706.1 (9) [Cu(**2**)$_2$(−H)]$^+$, 806.1 (3) [Cu(**2**)$_2$(ClO$_4$)]$^+$.

**Bis[bis[(*R*,*R*)-1,2-bis(1-methylbenzimidazol-2-yl)-1,2-ethanediol]cobalt(II) diperchlorate, [Co(*RR*-2)(*RR*-2-H)]$_2$(ClO$_4$)$_2$-(C$_2$H$_5$OH)$_3$(H$_2$O)$_2$.** A mixture of Co(ClO$_4$)$_2{\cdot}6$H$_2$O (0.0732 g, 0.2 mmol) and *RR*-**2** (0.1464 g, 0.4 mmol) was dissolved in 20

**Table 4** Crystal structures

| Compound | [Cu(*SS*-**1**)$_2$]$_2$(ClO$_4$)$_4$-(CH$_3$CN)$_4$(CH$_2$Cl$_2$) | [Cu(*SS*-**2**)$_2$](ClO$_4$)$_2$-(CH$_3$OH)(H$_2$O)$_{1.5}$ | *rac*-[Ni(*RR*,*SS*-**1**)$_2$](NO$_3$)$_2$-(C$_2$H$_5$OH)$_2$ | [Ni$_2$(*RR*-**2**)$_3$(*RR*-**2**-H)$_2$]-(ClO$_4$)$_2$(C$_2$H$_5$OH)$_3$ | [Ni(*SS*-**2**-H)$_2$](H$_2$O)$_4$]-(C$_2$H$_5$OH) |
|---|---|---|---|---|---|
| Formula | $C_{73}H_{70}N_{20}Cu_2Cl_6O_{24}$ | $C_{37}H_{43}N_8CuCl_2O_{14.5}$ | $C_{36}H_{38}N_{10}NiO_{12}$ | $C_{78}H_{88}N_{16}Ni_2Cl_2O_{19}$ | $C_{38}H_{48}N_8NiO_9$ |
| $M$ | 1951.3 | 966.3 | 861.5 | 1741.9 | 819.7 |
| Crystal system | Triclinic | Monoclinic | Monoclinic | Orthorhombic | Trigonal |
| Space group | $P\bar{1}$ | $C2$ | $C2/c$ | $C222_1$ | $P3_121$ |
| $a$/Å | 11.296(1) | 23.768(2) | 22.6083(11) | 17.1566(8) | 13.1970(5) |
| $b$/Å | 12.335(1) | 11.3948(7) | 11.5953(7) | 20.6583(9) | 13.1970(5) |
| $c$/Å | 16.357(1) | 16.5706(12) | 15.0449(7) | 24.1454(15) | |
| | | | | 21.1154(10) | |
| $\alpha$/° | 70.279(5) | 90 | 90 | 90 | 90 |
| $\beta$/° | 77.976(5) | 93.839(9) | 96.565(6) | 90 | 90 |
| $\gamma$/° | 76.047(6) | 90 | 90 | 90 | 120 |
| $V$/Å$^3$ | 2061.9(3) | 4477.8(5) | 3918.2(4) | 8557.8(8) | 3184.8(2) |
| $Z$ | 1 | 4 | 4 | 4 | 3 |
| $\mu$/mm$^{-1}$ | 3.189 (Cu-K$\alpha$) | 0.68 (Mo-K$\alpha$) | 0.57 (Mo-K$\alpha$) | 0.58 (Mo-K$\alpha$) | 0.52 (Mo-K$\alpha$) |
| Reflections measured | 9416 | 24376 | 24771 | 54114 | 35373 |
| Independent reflections ($R_{int}$) | 9416 | 8597 (0.06) | 3808 (0.041) | 8342 (0.077) | 4129 (0.055) |
| Flack parameter[22] | 0.01(2) | 0.05(3) | | 0.00(3) | −0.02(3) |
| $R$ indices [$\|F_o\| > 4\sigma(F_o)$] | 0.044, 0.056 | 0.066, 0.076 | 0.040, 0.043 | 0.047, 0.051 | 0.046, 0.055 |
| $R^a$, $\omega R^b$ | | | | | |
| Weights, $p^c$ | 0.0005 | 0.0004 | 0.0001 | 0.0004 | 0.0003 |

$^a$ $R = \Sigma||F_o| - |F_c||/\Sigma|F_o|$. $^b$ $\omega R = \{\Sigma[\omega(F_o^2 - F_c^2)^2]/\Sigma[\omega(F_o^2)^2]\}^{1/2}$. $^c$ $\omega = 1/[\sigma^2(F_o) + p(F_o)^2]$.

ml hot ethanol. After adding one equivalent sodium hydroxide (200 μl of 1 M NaOH, 0.2 mmol) a rose microcrystalline precipitate was formed. The cold solution was filtered and the microcrystalline powder vacuum dried (0.1464 g, 82%). Monocrystals suitable for X-ray structure analysis were obtained by dissolving $Co(ClO_4)_2 \cdot 6H_2O$ (0.0732 g, 0.2 mmol) and *RR*-**2** (0.1464 g, 0.4 mmol) in 60 ml ethanol. Slow evaporation led to rose crystals within 2 weeks (0.0194 g, 22%); (Found: C, 52.92; H, 5.18; N, 12.60. $C_{72}H_{70}N_{16}O_8 \cdot 2Co \cdot 2ClO_4 \cdot 2H_2O \cdot 3C_2H_6O$ requires C, 52.68; H, 5.21; N, 12.60%); UV ($T$ = 22 °C/0.0065 M/$CH_3CN$) $\lambda_{max}$/nm ($\varepsilon$/dm$^3$ mol$^{-1}$ cm$^{-1}$) 476 (35), 525 (22), 1053 (13); CD ($T$ = 22 °C/0.015 M/$CH_3CN$) $\lambda_{max}$/nm ($\Delta\varepsilon$/dm$^3$ mol$^{-1}$ cm$^{-1}$) 449 (−0.233), 491 (−0.110), 519 (−0.159). Reflectivity in MgO $\lambda_{min}$/nm 476, 525sh, 1057; IR (KBr) $\nu$/cm$^{-1}$ 3395br s, 2951w, 2878w, 1615m, 1480s, 1454m, 1414m, 1326m, 1287m, 1236m, 1147m, 114s, 1083s, 1009m, 928m, 834m, 813m, 746s, 686w, 625m, 563w, 546w, 504w, 442w, 429w; ES-MS (acetonitrile) $m/z$ (%) 323.2 (100) $[(\mathbf{2})H]^+$, 541.2 (42) $[Co_2(\mathbf{2})_3(-2H)]^{2+}$, 702.2 (16) $[Co_2(\mathbf{2})_4(-2H)]^{2+}/[Co(\mathbf{2})_2(-1H)]^+$, 859.2 (14) $[Co_2(\mathbf{2})_2(-2H)(ClO_4)]^+$, 759.1 (10) $[Co_2(\mathbf{2})_2(-3H)]^+$, 1181.2 (9) $[Co_2(\mathbf{2})_3(-2H)(ClO_4)]^+$, 1503.2 (<3) $[Co_2(\mathbf{2})_4(-2H)(ClO_4)]^+$; $^1$H-NMR (300 MHz) well resolved hyperfine shifted signals in the 100 to −80 ppm chemical shift range ($T$ = 20 °C/acetonitrile/$\delta$/ppm) 101.44(1H, s), 77.26 (1H, s), 33.89 (3H, s, $CH_3$), 21.73 (1H, s, arom. H), 20.20 (1H, s, arom. H), 8.41 (3H, s, $CH_3$), −5.66 (1H, s, arom. H), −9.55 (1H, s, arom. H), −13.20 (1H, s, arom. H), −22.43 (1H, s, arom. H), −65.42 (1H, s), −96.42 (1H, s).

### Crystal structure analysis

Data were collected at 200 K using a Stoe IPDS diffractometer except for $[Cu(SS\text{-}\mathbf{1})_2]_2(ClO_4)_4(CH_3CN)_4(CH_2Cl_2)$ where a Stoe STADI4 diffractometer was used. The structures were solved using MULTAN 87[21] and refined using the XTAL 3.2 set of programs.[22] For the non-racemic compounds the Flack absolute structure parameter[23] was refined. Some disorder of solvent and anion molecules was observed. Crystal data are summarised in Table 4.

CCDC reference numbers 183161–183165.

See http://www.rsc.org/suppdata/dt/b2/b203229e/ for crystallographic data in CIF or other electronic format.

## Acknowledgements

This work was supported by the Swiss National Science Foundation.

## References

1 P. Chaudhuri and K. Wieghardt, *Prog. Inorg. Chem.*, 1987, **35**, 329–436 (S. J. Lippard, ed.).
2 S. Trofimenko, *Scorpionates – The Coordination Chemistry of Polypyrazolylborate Ligands*, Imperial College Press, London, 1999.
3 C. Bolm, N. Meyer, G. Raabe, T. Weyermüller and E. Bothe, *Chem. Commun.*, 2000, 2435.
4 M. A. Phillips, *J. Chem. Soc.*, 1928, 172.
5 L. L.-Y. Wang and M. M. Joullié, *J. Am. Chem. Soc.*, 1957, 5706.
6 K. H. Taffs, L. V. Prosser, F. B. Wigton and M. M. Joullié, *J. Org. Chem.*, 1961, **26**, 462.
7 W. R. Roderick, C. W. Nordeen Jr, A. M. v. Esch and R. N. Appell, *J. Med. Chem.*, 1972, **15**, 655.
8 Y. Tong and M. Ding, *Youji Huaxe*, 1990, **10**, 464.
9 A. Tavman, B. Ulkuseven and N. M. Agh-Atabay, *Transition Met. Chem.*, 2000, **25**, 324.
10 B. Ülküsevev and A. Tavman, *Transition Met. Chem.*, 2001, **26**, 723.
11 G. A. v. Albada, J. Reedijk, R. Hämäläinen, U. Turpeinen and A. L. Spek, *Inorg. Chim. Acta*, 1989, **163**, 213.
12 V. Broughton, G. Bernardinelli and A. F. Wiliams, *Inorg. Chim. Acta*, 1998, **275–276**, 279.
13 M. L. Scudder, H. A. Goodwin and I. G. Dance, *New. J. Chem.*, 1999, **23**, 695.
14 W. Plass, A. Pohlmann and J. Rautengarten, *Angew. Chem., Int. Ed.*, 2001, **40**, 4207.
15 C. K. Jørgensen, *Modern Aspects of Ligand Field Theory*, North-Holland Publishing Company, Amsterdam, 1971.
16 D. A. Evans, M. C. Kozlowski, J. A. Murry, C. S. Burgey, K. R. Campos, B. T. Connell and R. J. Staples, *J. Am. Chem. Soc.*, 1999, **121**, 669.
17 K. Bernauer, S. Bourqui, D. Hugi-Cleary and R. Warmuth, *Helv. Chim. Acta*, 1992, **75**, 1288.
18 A. D. Zuberbühler and T. A. Kaden, *Talanta*, 1982, **29**, 201.
19 O. Kahn, *Molecular Magnetism*, VCH, Weinheim, 1993.
20 W. C. Wolsey, *J. Chem. Educ.*, 1973, **50**, A335.
21 P. Main, S. J. Fiske, S. E. Hull, L. Lessinger, D. Germain, J. P. Declercq, and M. M. Woolfson, in 'MULTAN 87', 1987.
22 S. R. Hall, H. D. Flack and J. M. Stewart, XTAL 3.2 User's Manual, Universities of Western Australia, Geneva and Maryland, 1992.
23 (*a*) H. D. Flack and G. Bernadinelli, *Acta Crystallogr., Sect. A*, 1999, **55**, 908; (*b*) H. D. Flack and G. Bernadinelli, *J. Appl. Crystallogr.*, 2000, **33**, 1134.